Optical reflectivity of solid and liquid methane: Application to spectroscopy of Titan's hydrocarbon lakes

Kimberly A. Adams,[1] Steven D. Jacobsen,[1] Zhenxian Liu,[2] Sylvia-Monique Thomas,[1,3] Maddury Somayazulu,[2] and Donna M. Jurdy[1]

Received 18 September 2011; revised 24 October 2011; accepted 25 October 2011; published 29 February 2012.

[1] Reflectance spectroscopy of outer solar system bodies provides direct observations for interpreting their surface compositions. At Titan, the *Cassini* spacecraft revealed dark patches in the surface reflectance at 2 and 5 μm, interpreted as hydrocarbon lakes forming seasonally through a methane cycle. Whereas the composition of planetary materials in the solar system has been inferred from characteristic absorption bands, identification of phase states (liquid versus solid) on dynamic planetary surfaces requires laboratory reflectance ratio measurements at relevant temperatures. Using visible and near-infrared radiation from the National Synchrotron Light Source (NSLS), reflectance ratios of solid (single crystal) versus liquid CH_4 were measured at temperatures from 50–100 K. Although the wavelength and shape of the characteristic methane absorption bands at around 1.7 and 2.3 μm are insensitive to temperature or phase state from 50–100 K, the broad-spectrum reflectivity $R(\lambda)$ at 0.5–2 μm decreases dramatically upon melting by at least 25% at 87–94 K. Transition from solid CH_4-I to liquid states at ~90 K displays a reflectance ratio R_{solid}/R_{liq} 1.3–1.6 at 2 μm. This darkening of CH_4 upon melting at 87–94 K is similar at visible wavelengths, and consistent with observations of hydrocarbon lakes in the far northern and southern latitudes of Titan. **Citation:** Adams, K. A., S. D. Jacobsen, Z. Liu, S.-M. Thomas, M. Somayazulu, and D. M. Jurdy (2012), Optical reflectivity of solid and liquid methane: Application to spectroscopy of Titan's hydrocarbon lakes, *Geophys. Res. Lett.*, *39*, L04309, doi:10.1029/2011GL049710.

1. Introduction

[2] Solid methane is abundant on the surfaces of icy bodies in the outer Solar System including Triton [e.g., *Apt et al.*, 1983; *Cruikshank et al.*, 1993], Pluto [e.g., *Cruikshank et al.*, 1976; *Owen et al.*, 1993; *Grundy and Fink*, 1996], and other large trans-Neptunian objects [e.g., *Brown et al.*, 2005; *Licandro et al.*, 2006; *Brown et al.*, 2007] as identified in observational spectra from characteristic absorption bands in the visible or infrared (IR) spectral range. Laboratory spectra of light hydrocarbon ices, typically measured by transmission in the near or mid-IR [e.g., *Grundy et al.*, 2002; *Hudson et al.*, 2009] provide insight into the chemical compositions of planetary surfaces. However, the physical state (liquid versus solid) of CH_4 and other hydrocarbons in the Solar System cannot be readily interpreted from the absorption band positions alone due to the similarity between spectra of liquid, amorphous, and disordered crystalline states.

[3] Recent discoveries of lakes on Titan from the *Cassini* mission are interpreted from a combination of low-lying and flat surfaces measured by Radar [*Stofan et al.*, 2007; *Hayes et al.*, 2008] and corresponding dark features observed in near-IR (~2 μm) reflectance ratios of spectra from inside and outside the lake areas using the Visual and Infrared Mapping Spectrometer (VIMS) [*Brown et al.*, 2008]. Therefore, interpretation of recent and forthcoming mission observations of outer Solar System objects requires laboratory reflectance spectroscopy of planetary ices and liquids at relevant temperatures, and wavelength, especially to distinguish states of phases on dynamic planetary surfaces.

[4] Since Voyager, considerable interest has focused on Titan's surface composition, thought to be near the triple point of methane [*Sagan and Dermott*, 1982; *Lunine et al.*, 1983]. Recently, the *Huygens* probe (at 10.3°S, 192.4°W) measured a temperature of 93.6 K and pressure of 1,467 hPa (~1.5 bars), confirming that coexisting states of CH_4 could persist on Titan's surface and lower atmosphere [*Fulchignoni et al.*, 2005]. Titan's methane cycle [*Samuelson and Mayo*, 1997; *Tokano et al.*, 2001; *Atreya et al.*, 2005; *Niemann et al.*, 2005; *Atreya et al.*, 2006; *Mitri et al.*, 2007; *Hayes et al.*, 2008; *Lunine and Atreya*, 2008] is therefore analogous to the Earth's hydrologic cycle, where rain and clouds of methane exchange with solid and liquid methane on the surface. To more fully understand Titan's methane cycle, additional tools are required to identify the states of planetary materials from spectroscopic observation.

[5] Previous studies of liquid methane include transmission spectra in the far-infrared (15–1000 μm) at 98–100 K [*Savoie and Fournier*, 1970; *Arning et al.*, 1981; *Weiss et al.*, 1969], near to mid-infrared absorption studies at 0.6–2 μm [*Ramaprasad et al.*, 1978] and 0.7–5 μm [*Grundy et al.*, 2002], as well as in the visible [*Patel et al.*, 1980]. Reflectance spectra of liquid methane have been reported at 98 K for mid-to-long wavelength IR from 2.5–20 μm [*Pinkley et al.*, 1978]. Near-IR reflectance spectra of liquid and solid methane at 88–100 K are needed within the 2 μm window used by *Brown et al.* [2008] to predict reflectance ratios for solid–liquid methane on Titan.

[6] Previous studies of solid CH_4-I methane include transmission studies in the far-IR at 77 K [*Savoie and Fournier*, 1970] and 30 K [*Orbriot et al.*, 1978]. Covering the near-to-mid IR range from 1–22 μm, *Pearl et al.* [1991] measured

[1]Department Earth and Planetary Sciences, Northwestern University, Evanston, Illinois, USA.
[2]Geophysical Laboratory, Carnegie Institution of Washington, Washington, D. C., USA.
[3]Now at Department of Geoscience, University of Nevada, Las Vegas, Las Vegas, Nevada, USA.

0094-8276/12/2011GL049710

absorbance in CH_4-I thin films (~1–200 μm thick) at 30 K. Thicker samples (1–11 mm) of CH_4-I at 27 K were used in a study to reveal weaker absorbance bands in the near-IR at 0.8–2.5 mm by *Calvani et al.* [1992]. The temperature dependence of CH_4-I ice absorption spectra were measured between 30 and 90 K from 0.7–5 μm by *Grundy et al.* [2002], who in addition, obtained absorbance of liquid methane at 93 K. *Grundy et al.* [2002] identify some temperature-dependent changes in the peak shape (width) of various absorption bands in the near-IR. However, there is an unfortunate similarity in solid–liquid methane spectra, especially in absorbance band positions, that arises from the fact that CH_4-I ice is cubic and rotationally disordered. Therefore, from absorption bands alone it may be nearly impossible to distinguish crystalline from liquid CH_4.

[7] In this study, we measured the visible and near-IR reflectance of liquid and solid CH_4 in the temperature range of 50–100 K and spectral range of 0.6–0.8 μm and 1.4–2.5 μm paying attention to the broad-spectrum reflectance ratio upon melting of solid CH_4-I ice at about 92 K. The in-situ optical reflectivity measurements were conducted through the triple point of methane using a confocal optical system in conjunction with a diamond-anvil optical cell [e.g., *Syassen and Sonnenschein*, 1982]. The measured reflectance ratio of solid/liquid methane is consistent with VIMS observations of hydrocarbon lakes in the far northern and southern latitudes of Titan.

2. Methods

[8] A symmetric diamond-anvil cell (DAC) was used as an optical sample holder to contain the methane sample. The method of collecting confocal reflectivity spectra in a DAC follows *Syassen and Sonnenschein* [1982] and *Seagle et al.* [2009]. The optical cell was fitted with type-I diamond anvils faceted with 400 μm flat culets. A sample chamber was formed by drilling a 250 μm diameter hole into a 250 μm thick stainless steel foil, pre-indented by the anvils to about 100 μm thickness, which formed a tight gasket between the anvils. A small annealed ruby sphere was also loaded into the sample chamber to act as a pressure marker during the measurements using laser-excited ruby fluorescence [*Mao et al.*, 1986].

[9] Pure CH_4 was compressed into the DAC at around 170 MPa (1.7 kbar) in the gas-loading system at the Geophysical Laboratory, Carnegie Institution of Washington. In order to confirm that the sample was loaded without contamination, Raman spectra were obtained at 300 K after loading and indicated that the sample chamber contained pure CH_4, nominally free of grease, water, or similar contaminants. According to the ruby pressure marker in the cell, the pressure of the sample during the optical measurements was 0.02–0.06 GPa (0.2–0.6 kbar). Because the measured ruby pressure was less than 1 kbar, the CH_4-I phase of methane ice was stable on solidification of the sample for measurements below 93 K, rather than CH_4-II or CH_4-III, which would be stable at pressures >4 kbar and T > 50 K [e.g., *Orbriot et al.*, 1978].

[10] The methane-filled DAC was loaded into a helium-cooled cryostat on the U2A beamline of the NSLS, Brookhaven National Laboratory. The DAC was initially cooled to below 93 K to observe the solidification of methane from coexisting liquid and vapor (Figure 1). On cooling, the CH_4 vapor bubble remained present until crystallization was observed just below 94 K (Figure 1). Prior to solidification of the sample, the size of the vapor bubble remained constant during the cooling process, indicating that the system was isochoric during cooling. After cooling to 50 K, the sample was brought back to 180 K for several hours and then cooled to 100 K before commencing the optical measurements under decreasing temperatures. IR-reflectivity measurements were made at 5–10 K temperature increments between 100 and 50 K, with two measurements for methane in the liquid phase, and seven spectra in the solid phase.

[11] The optical experiments performed at NSLS were made on a Bruker IFS 66v/S Fourier transform infrared (FTIR) spectrometer using a mid-band MCT IR-detector and a custom-built, confocal microscope with all-reflecting optics. Near-IR spectra were obtained between 0.91 μm and 3.84 μm. However, due to low detector sensitivity below ~1.4 μm and high absorbance from diamond above ~2.5 μm, the usable spectral range was limited to 1.4–2.5 μm. Visible reflectance was obtained using a tungsten lamp source, Princeton Instruments spectrograph with 500 mm focal length, and N_2-cooled CCD detector. Measurements were made between 0.4 μm and 1.09 μm. Due to strong diamond absorbance below 0.6 μm and non-linear detector sensitivity above ~0.8 μm the usable range was cut to 0.6–0.8 μm for our estimates of reflectance ratios.

[12] At each temperature, before focusing light onto the sample, the intensity from the air-diamond interface (I_d) was measured. Intensities from the sample diamond interface (I_{sd}) were normalized to I_d to correct for the decaying storage-ring current between electron injections of the VUV (vacuum ultra-violet) ring at NSLS. The reflectivity of the sample-diamond interface (R_{sd}) was further treated for optical properties of the cell following the procedure of *Seagle et al.* [2009], shown schematically in Figure 2, with:

$$R_{sd}(\lambda) = (I_{sd}/I_e)^*(I_d/I_0) \quad (1)$$

where I_{sd} is the intensity reflected from the sample-diamond interface, I_e is the intensity reflected from the culet of an empty cell, I_d is the intensity reflected from the air-diamond interface, and I_0 is the source intensity. The ratio I_d/I_0 is the reflectivity of the diamond anvil window, which is approximately 0.18 (±0.01) over the wavelength range of 0.6–2.5 μm, confirmed by many individual measurements on the U2A beamline at NSLS. The ratio I_e/I_d was measured in the near-IR range and found to be approximately 0.65 from 1.4–2.5 μm (Figure 2). Substituting $I_d/I_0 = 0.18$ (constant) and $I_e = 0.65I_d$ into equation (1), gives:

$$R_{sd} = [I_{sd}/(0.65^*I_d)]^*0.18 \quad (2)$$

where I_{sd} and I_d were measured at every temperature and as a function of wavelength in the visible through near-IR. Whereas we cannot obtain the reflectivity of the methane sample against air in this experimental setup, equation (2) provides an adequate way of determining the relative change in reflectivity of solid versus liquid methane at temperatures relevant to the surface of Titan. This is achieved by taking the ratio R_{solid}/R_{liquid} from each of the R_{sd} values, at about 2 μm.

3. Results

[13] Because the wavelength range in the current study is narrow, extending from ~0.6–0.8 μm in the visible and from

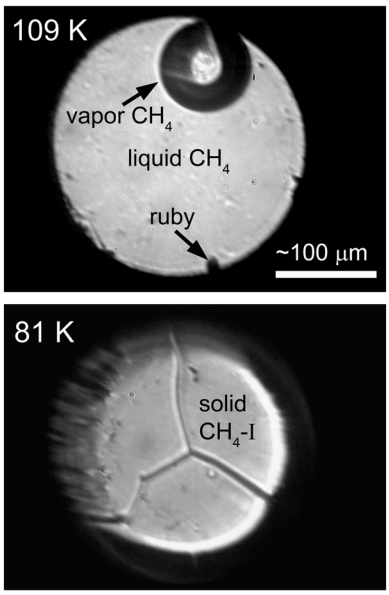

Figure 1. Optical micrograph of CH_4 (top) at 109 K and (bottom) at 81 K during cooling and solidification of methane, which was observed at around 90 K.

1.4–2.5 μm in the near-IR, it is beyond the scope of the current study to determine quantitative optical constants of liquid and solid methane from Kramers-Kronig analysis. However, because previous reflectance measurements of methane (liquid only) extend from 2.5–25 μm [*Pinkley et al.*, 1978], here we intend to extend reflectance measurements down to 2.5–1.4 μm in order to cover the 2.0 μm atmospheric window used by the VIMS team [*Brown et al.*, 2007] to construct reflectance ratios around Titan's Ontario Lacus. We focus on determining the ratio of reflectance between solid and liquid forms of CH_4 at 87–93 K with application to interpreting recent and forthcoming VIMS reflectance ratios of Titan's hydrocarbon lakes.

[14] Near-IR reflectivity of solid and liquid methane from 50–100 K are shown in Figure 3. Consistent with previous absorption measurements [*Grundy et al.*, 2002] we observe three sharp absorption bands at 1.6–1.8 μm and three sharp absorption bands at 2.2–2.4 μm. The positions of these absorption bands do not vary with state (solid versus liquid) or temperature. However, between 87 and 94 K, the reflectivity of methane dramatically decreases upon transition from the solid to the liquid state. At 2 μm, $R_{sd} = 0.175$ for solid methane at 87 K (green spectrum in Figure 3) and decreases to $R_{sd} = 0.132$ for liquid methane at 94 K (black spectrum in Figure 3). The ratio, $R_{solid}/R_{liquid} = 1.32$ at these temperatures represents the minimum contrast between liquid and solid CH_4 at 2 μm. Although the broad reflectivity values of liquid methane between 1.6 and 2.5 μm do not vary systematically with temperature, the maximum contrast was observed between the spectrum of liquid CH_4 at 94 K and solid CH_4 at 60 K, with $R_{sd} = 0.22$ (pink spectrum in Figure 3). The contrast between liquid methane at 94 K and solid methane at 60 K is $R_{solid}/R_{liquid} = 1.67$.

[15] The visible reflectance of solid and liquid methane is also shown in Figure 3. In the visible region, interference fringes resulting from reflections within the DAC were observed for the liquid state but are minimal upon transition to solid methane between 87 and 94 K. For the purpose of estimating R_{solid}/R_{liquid} at visible wavelengths, we fit polynomial curves through the data to approximate the value of R_{sd} (solid curves in Figure 3). Similar to the near-IR results, we observe a decrease in the sample reflectance at the diamond interface (R_{sd}) during transitions from solid to liquid. The visible reflectance at 87 K for solid methane is 0.232, and decreases to 0.183 for liquid methane at 94 K. The contrast at 87–94 K between solid and liquid methane is $R_{solid}/R_{liquid} = 1.27$, similar to the near-IR results.

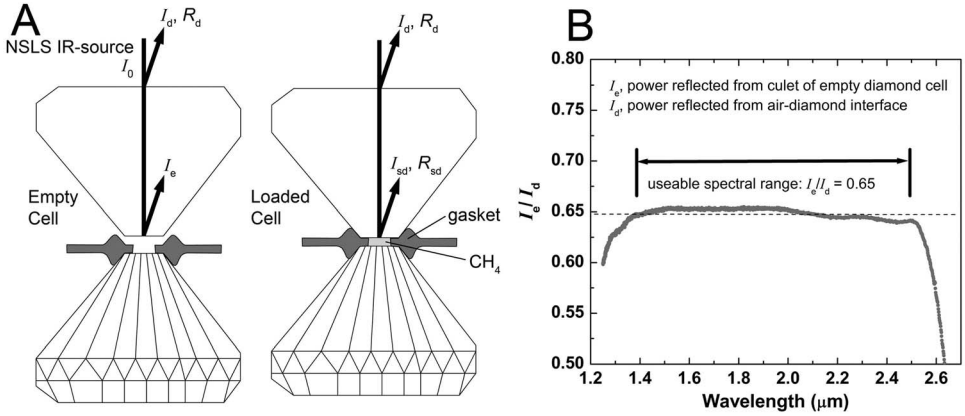

Figure 2. (a) Schematic of the reflectivity measurements made in a DAC following the procedure of *Seagle et al.* [2009]. R_{sd} is the reflectivity of the sample-diamond interface, normalized to the incident beam intensity and corrected for the reflectivity of the diamond window (equations (1) and (2)). I_{sd} is the intensity reflected from the sample-diamond interface, I_d is the intensity reflected from the air-diamond interface, I_e is the intensity reflected from the culet of the empty cell, and I_0 is the source intensity. (b) Measured ratio, I_e/I_d of a diamond anvil is approximately constant over the current experimental wavelength range. The ratio gives the power reflected from the diamond culet, $I_e = 0.65I_d$, and was used to calculate the reflectivity of the sample-diamond interface, R_{sd} (equation (2)).

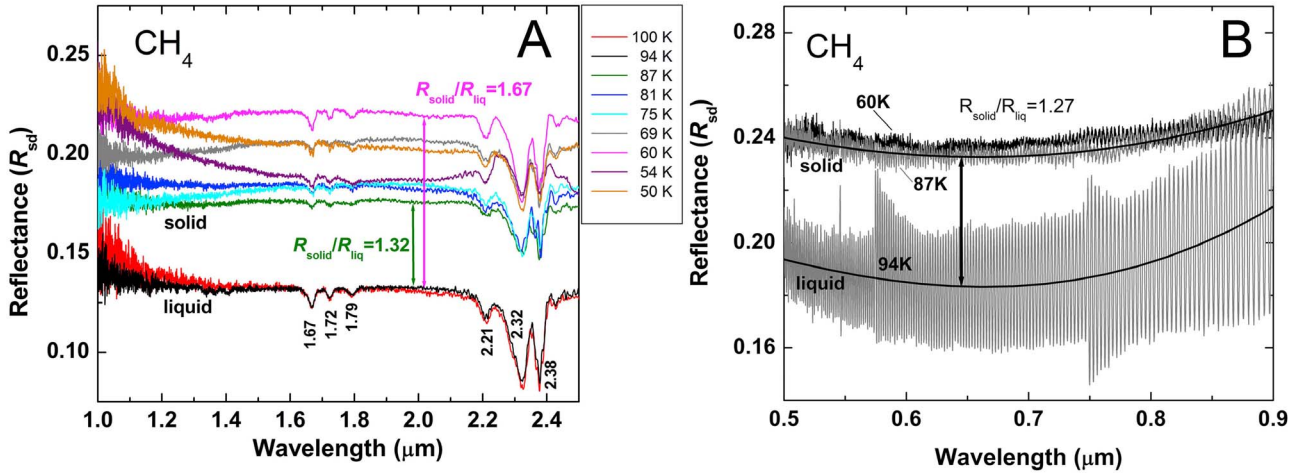

Figure 3. (a) Near-IR reflectance of methane at the sample-diamond interface (R_{sd}) as a function of temperature. Spectra obtained at 100 and 94 K are from the liquid phase and at 87 K and below the sample was single crystal CH_4. The labeled peak positions of characteristic absorbance bands of methane were essentially unchanged over this temperature range, however the ratio of reflectance of the solid phase to the liquid phase was 1.32–1.67 indicating a significant darkening of liquid methane at 2 μm. (b) Visible reflectance of methane at the sample-diamond interface (R_{sd}) as a function of temperature. Interference fringes in the visible region result from internal reflections in the diamond-anvil cell. The solid curves show a polynomial fit to the data, from which we infer a ratio of R_{solid}/R_{liquid} of about 1.27 at 0.65 μm between 94 and 87 K.

[16] Using equations (1) and (2) we correct for the reflectivity of the diamond anvil, and by normalizing every sample measurement to I_d, we correct for the decaying synchrotron storage ring current. Even with these corrections, the measurement of reflectance in the current setup with a diamond-sample interface needs to be directly compared with sample-air reflectivity for validation. Experiments on other materials (such as gold) are ongoing at U2A of the NSLS to evaluate the difference between the corrected reflectance at the sample-diamond interface (R_{sd}) and R, the sample reflectance against air. Although preliminary results suggest that the diamond window corrections are valid because the ratio I_e/I_d (for the empty cell) is constant, we stress the value of sample reflectance ratios (R_{solid}/R_{liquid}) rather than absolute reflectance.

[17] By containing the methane sample in a DAC, samples were measured at a maximum pressure of 50 MPa, compared with the 1,467 hPa pressures of Titan's surface [*Fulchignoni et al.*, 2005]. However, the pressure dependence of methane reflectivity is minimal over the 50 MPa pressure range of the sample in this DAC experiment. *Sun et al.* [2006] have shown that the pressure dependence of the refractive index changes by only 0.00268/GPa. Therefore, within our 50 MPa range of pressure we expect a change in the refractive index of only 0.00134, which is not enough to influence our results. We are also confident the experiment was performed at pressures below the critical density of CH_4 due to the observation of a vapor bubble coexisting with liquid.

[18] The value of R_{sd} for liquid methane from this study may be directly comparable to Titan's lakes, however we hesitate to compare R values from the solid-CH_4 due to the strong grain size dependence of R [e.g., *Kieffer*, 1990]. By noting the grain boundaries of solid methane in Figure 1 and the gasket hole size of 250 μm, we estimate a grain size of 100 μm. However, this optical setup is confocal, where light is collected from an isolated focal plane within the sample. Specifically, we used a 20 μm aperture for the incident synchrotron beam and the confocal aperture was about 10 μm, both significantly less than the $\sim$100 μm grain size of solid CH_4 in this study (Figure 1). We therefore conclude that our values of reflectance for solid methane are essentially from a single crystal. Because reflectance increases with decreasing grain size in ices such as H_2O [e.g., *Kieffer*, 1990], the current single crystal measurements should represent a maximum contrast in reflectance between the solid and liquid phase, R_{solid}/R_{liquid}.

4. Discussion

[19] The reflectivity ratio of solid versus liquid methane has been determined at temperatures relative to the surface of Titan in order to evaluate recent and forthcoming *Cassini* observations of Titan's possible hydrocarbon lakes. The study of *Brown et al.* [2008] focused attention on surface reflectivity within several bands of relative transparency in Titan's atmosphere at 1.6, 2.0, and 5.0 μm. Specifically, observations across Ontario Lacus in the southern hemisphere revealed a dark structure corresponding to the low-lying and flat radar structure of Ontario Lacus [*Wye et al.*, 2009]. Similarly, in the northern latitudes, large lake-like features coincide with corresponding radar and dark reflectance as measured by VIMS.

[20] Although direct comparisons of brightness variations across Ontario Lacus are not possible at this time due to the non-normal viewing angle of measurements made by Cassini, clearly there is a darkening of the lake's interior compared to the surrounding "beach" area at about 2 μm. This is consistent with the darkening observed in our methane laboratory reflectance measurements at the same

wavelength, which show a ratio of solid/liquid methane of 1.32–1.67. As normal reflectance data from Titan's surface is extracted from Cassini spectral observations in the future, laboratory reflectance ratios will be necessary to determine the physical state of lakes on Titan.

[21] The reflectance of solids is strongly grain-size dependent [e.g., *Kieffer*, 1990] where increases in reflectivity are observed as grain size decreases. Our confocal observations are essentially single crystal, thus our R_{solid}/R_{liquid} values represent a maximum contrast. A two-fold increase in reflectance for a polycrystalline surface of ethane or methane would not be unreasonable. We therefore conclude that observed solid/liquid reflectance ratios of CH_4 at Titan's surface temperatures are consistent with the hydrocarbon lake observations from VIMS. Because the dominant compound in Titan's lakes is likely ethane with minor amounts of methane [*Brown et al.*, 2008], similar experiments on ethane and ethane-methane mixtures are underway.

[22] The measured surface temperature of Titan from *Huygens* landing was 93.65 K [*Fulchignoni et al.*, 2005]. Temperatures near the poles reach approximately 90.5 K at 87°N and 91.7 K at 88°S [*Jennings et al.*, 2009]. In our experiments, we observed crystallization of co-existing liquid and vapor CH_4 (Figures 1 and 3) between 87 and 94 K, confirming that Titan's surface conditions coincide with the triple point of methane, and thus the likelihood that clouds, rain, and lakes of methane exchange with the solid surface of Titan much in the way Earth's hydrologic cycle operates.

[23] **Acknowledgments.** This research was supported by a Fellowship from the David and Lucile Packard Foundation to SDJ, US National Science Foundation award EAR-0748707 (CAREER) to SDJ, and by the DOE-BES to MSS. Use of the National Synchrotron Light Source (NSLS), Brookhaven National Laboratory, was supported by the U.S. Department of Energy, Office of Science, Office of Basic Energy Sciences, under Contract No. DE-AC02-98CH10886. Operation of beamline U2A at the NSLS is supported by COMPRES, the Consortium for Material Properties Research in the Earth Sciences under NSF Cooperative Agreement grant EAR 06–49658, and by the U.S. Department of Energy through the Carnegie/DOE Alliance Center (CDAC) contract DE-FC03-03 N00144. KAA acknowledges support from CDAC, NSF, and COMPRES.

[24] The Editor thanks the two anonymous reviewers for their assistance in evaluating this paper.

References

Apt, J., N. P. Carleton, and C. D. Mackay (1983), Methane on Triton and Pluto: New CCD spectra, *Astrophys. J.*, *270*, 342–350, doi:10.1086/161127.

Arning, H. J., K. Tibulski, and T. Dormuller (1981), Collision-induced spectra of simple liquids, *Ber. Bunsenges. Phys. Chem.*, *85*, 1068–1071.

Atreya, S. K., H. B. Niemann, T. C. Owen, E. Y. Adams, and J. E. Demick, and the GCMS Team (2005), Methane on Titan: Photochemical-meteorological-hydrochemical cycle, *Bull. Am. Astron. Soc.*, *37*, 735.

Atreya, S. K., E. Y. Adams, H. B. Niemann, J. E. Demick-Montelara, T. C. Owen, M. Fulchignoni, F. Ferri, and E. H. Wilson (2006), Titan's methane cycle, *Planet. Space Sci.*, *54*, 1177–1187, doi:10.1016/j.pss.2006.05.028.

Brown, M. E., C. A. Trujillo, and D. L. Rabinowitz (2005), Discovery of a planetary-sized object in the scattered Kuiper belt, *Astrophys. J.*, *635*, L97–L100, doi:10.1086/499336.

Brown, M. E., K. M. Barkume, G. A. Blake, E. L. Schaller, D. L. Rabinowitz, H. G. Roe, and C. A. Trujillo (2007), Methane and ethane on the bright kuiper belt object 2005 FY9, *Astron. J.*, *133*, 284–289, doi:10.1086/509734.

Brown, R. H., L. A. Soderblom, J. M. Soderblom, R. N. Clark, R. Juamann, J. W. Barnes, C. Sotin, B. Buratti, K. H. Baines, and P. D. Nicholson (2008), The identification of liquid ethane in Titan's Ontario Lacus, *Nature*, *454*, 607–610, doi:10.1038/nature07100.

Calvani, P., S. Cunsolo, S. Lupi, and A. Nucara (1992), The near infrared spectrum of solid CH_4, *J. Chem. Phys.*, *96*(10), 7372–7379, doi:10.1063/1.462440.

Cruikshank, D. P., C. B. Pilcher, and D. Morrison (1976), Pluto: Evidence for methane frost, *Science*, *194*, 835–837, doi:10.1126/science.194.4267.835-a.

Cruikshank, D. P., T. L. Roush, T. C. Owen, T. R. Geballe, C. de Bergh, B. Schmitt, R. H. Brown, and M. J. Bartholomew (1993), Ices on the surface of Triton, *Science*, *261*, 742–745, doi:10.1126/science.261.5122.742.

Fulchignoni, M., et al. (2005), In situ measurements of the physical characteristics of Titan's environment, *Nature*, *438*, 785–791, doi:10.1038/nature04314.

Grundy, W. M., and U. Fink (1996), Synoptic CCD spectrophotometry of Pluto over the past 15 years, *Icarus*, *124*, 329–343, doi:10.1006/icar.1996.0208.

Grundy, W. M., B. Schmitt, and E. Quirico (2002), The temperature-dependent spectrum of methane ice I between 0.7 and 5 μm and opportunities for near-infrared remote thermometry, *Icarus*, *155*, 486–496, doi:10.1006/icar.2001.6726.

Hayes, A., et al. (2008), Hydrocarbon lakes on Titan: Distribution and interaction with a porous regolith, *Geophys. Res. Lett.*, *35*, L09204, doi:10.1029/2008GL033409.

Hudson, R. L., M. H. Moore, and L. L. Raines (2009), Ethane ices in the outer solar system: spectroscopy and chemistry, *Icarus*, *203*, 677–680, doi:10.1016/j.icarus.2009.06.026.

Jennings, D. E., et al. (2009), Titan's surface brightness temperatures, *Astrophys. J.*, *691*, L103–L105, doi:10.1088/0004-637X/691/2/L103.

Kieffer, H. H. (1990), H_2O grain size and the amount of dust in Mars' residual north polar cap, *J. Geophys. Res.*, *95*, 1481–1493, doi:10.1029/JB095iB02p01481.

Licandro, J., N. Alonso-Pinilla, M. Pedani, E. Oliva, G. P. Tozzi, and W. M. Grundy (2006), The methane ice rich surface of large TNO 2005 FY9: A Pluto-twin in the trans-neptunian belt?, *Astron. Astrophys.*, *445*, L35–L38, doi:10.1051/0004-6361:200500219.

Lunine, J. I., and S. K. Atreya (2008), The methane cycle on Titan, *Nat. Geosci.*, *1*, 159–164, doi:10.1038/ngeo125.

Lunine, J. I., D. J. Stevenson, and Y. L. Yung (1983), Ethane ocean on Titan, *Science*, *222*, 1229–1230, doi:10.1126/science.222.4629.1229.

Mao, H. K., J. Xu, and P. M. Bell (1986), Calibration of the ruby pressure gauge to 800 kbar under quasi-hydrostatic conditions, *J. Geophys. Res.*, *91*, 4673–4676, doi:10.1029/JB091iB05p04673.

Mitri, G., A. P. Showman, J. I. Lunine, and R. D. Lorenz (2007), Hydrocarbon lakes on Titan, *Icarus*, *186*, 385–394, doi:10.1016/j.icarus.2006.09.004.

Niemann, H. B., et al. (2005), The abundances of constituents of Titan's atmosphere from the GCMS instrument on the Huygens probe, *Nature*, *438*, 779–784, doi:10.1038/nature04122.

Orbriot, J., F. Fondere, P. Marteau, H. Vu, and K. Kobashi (1978), Far-infrared spectra of solid CH_4 under high pressure, *Chem. Phys. Lett.*, *60*(1), 90–94, doi:10.1016/0009-2614(78)85717-0.

Owen, T. C., T. L. Roush, D. P. Cruikshank, J. L. Elliot, L. A. Young, C. de Bergh, B. Schmitt, T. R. Geballe, R. H. Brown, and M. J. Bartholomew (1993), Surface ices and the atmospheric composition of Pluto, *Science*, *261*, 745–748, doi:10.1126/science.261.5122.745.

Patel, C. K. N., E. T. Nelson, and R. J. Kerl (1980), Opto-acoustic study of weak optical absorption of liquid methane, *Nature*, *286*, 368–370, doi:10.1038/286368a0.

Pearl, J., N. Ngoh, M. Ospina, and R. Khanna (1991), Optical constants of solid methane and ethane from 10,000 to 450 cm^{-1}, *J. Geophys. Res.*, *96*, 17,477–17,482, doi:10.1029/91JE01741.

Pinkley, L. W., P. P. Sethna, and D. Williams (1978), Optical constants of liquid methane in the infrared, *J. Opt. Soc. Am.*, *68*(2), 186–189, doi:10.1364/JOSA.68.000186.

Ramaprasad, K. R., J. Caldwell, and D. S. McClure (1978), The vibrational overtone spectrum of liquid methane in the visible and near infrared: Applications to planetary studies, *Icarus*, *35*(3), 400–409, doi:10.1016/0019-1035(78)90092-1.

Sagan, C., and S. F. Dermott (1982), The tide in the seas of Titan, *Nature*, *300*, 731–733, doi:10.1038/300731a0.

Samuelson, R. E., and L. A. Mayo (1997), Steady-state model for methane condensation in Titan's troposphere, *Planet. Space Sci.*, *45*, 949–958, doi:10.1016/S0032-0633(97)00089-5.

Savoie, R., and R. P. Fournier (1970), Far-infrared spectra of condensed methane and methane-d_4, *Chem. Phys. Lett.*, *7*, 1–3, doi:10.1016/0009-2614(70)80232-9.

Seagle, C. T., D. L. Heinz, Z. Liu, and R. J. Hemley (2009), Synchrotron infrared reflectivity measurements of iron at high pressures, *Appl. Opt.*, *48*, 545–552, doi:10.1364/AO.48.000545.

Stofan, E. R., et al. (2007), The lakes of Titan, *Nature*, *445*, 61–64, doi:10.1038/nature05438.

Sun, L. L., A. L. Ruoff, C. S. Zha, and G. Stupian (2006), Optical properties of methane to 288 GPa at 300K, *J. Phys. Chem. Solids*, *67*, 2603–2608, doi:10.1016/j.jpcs.2006.08.003.

Syassen, K., and R. Sonnenschein (1982), Microoptic double beam system for reflectance and absorption measurements at high pressure, *Rev. Sci. Instrum.*, *53*(5), 644–650, doi:10.1063/1.1137035.

Tokano, T., F. M. Neubauer, M. Laube, and C. P. McKay (2001), Three-dimensional modeling of the tropospheric methane cycle on Titan, *Icarus*, *153*, 130–147, doi:10.1006/icar.2001.6659.

Weiss, S., G. E. Leroy, and R. H. Cole (1969), Pressure-induced infrared spectrum of methane, *J. Chem. Phys.*, *50*, 2267, doi:10.1063/1.1671367.

Wye, L. C., H. A. Zebker, and R. D. Lorenz (2009), Smoothness of Titan's Ontario Lacus: Constraints from Cassini RADAR specular reflection data, *Geophys. Res. Lett.*, *36*, L16201, doi:10.1029/2009GL039588.

K. A. Adams, S. D. Jacobsen, and D. M. Jurdy, Department of Earth and Planetary Sciences, Northwestern University, Evanston, IL 60208, USA. (kadams@earth.northwestern.edu)

Z. Liu and M. Somayazulu, Geophysical Laboratory, Carnegie Institution of Washington, Washington, DC 20015, USA.

S.-M. Thomas, Department of Geoscience, University of Nevada, Las Vegas, Las Vegas, NV 89154, USA.